

Full Length Research Paper

Characterization of the aquifer system in the northern Sinai peninsula, Egypt

Mohamed ElKashouty^{1*}, Magdy Hosney ElSayed², Yehia El Godamy², Mohamed Gad² and Morquesd Mansour²

¹Department of Geology, Faculty of Science, Cairo University, Egypt.

²Desert Research Center, Matariya, Egypt.

Accepted 27 June, 2011

Northern Sinai has received great attention with respect to future agricultural development, especially after initiation of El Salam canal, as a source of irrigation. The research aim is to highlight on the nature and potentiality of the Quaternary aquifer in the northern Sinai. To achieve this target, a 256 groundwater samples were collected and analyzed chemically with respect to major ions, SiO₂, B³⁺, PO₄³⁻, NO₃⁻, Br⁻, I⁻, Pb²⁺, Fe³⁺, Cd²⁺, Ni²⁺, Cu²⁺, Zn²⁺, and Co²⁺. Five infiltration tests were accomplished at five soil sites. Two pumping and one reanalyzed tests were carried out to determine the hydrogeological parameters of the Quaternary aquifer. The granulometric investigation was measured for 15 sub soils of five soil sites. The total dissolved solids (TDS) concentration of the Quaternary aquifer is increased in the northern part of the sub area A. It reflects the impact of seawater intrusion. In the sub area B, the TDS concentration is decreased towards the northern part, due to recharge from El Salam canal (fresh water). There is hydrogeological interconnection between El Salam canal and aquifer system in the northern Sinai. In sub area C, the TDS concentration is increased towards the northwestern part (Suez canal), caused by seawater intrusion from Suez Canal. The PO₄³⁻, NO₃⁻ and most of the toxic metals (Pb²⁺, Fe³⁺, Mn²⁺, Cd²⁺, Ni²⁺, Cu²⁺, Zn²⁺ and Co²⁺) concentrations in groundwater were recorded in medium to high concentrations in sub areas (B and C). It attributes to leakage of septic tank, seepage from El Salam canal, agricultural activity and geomeia. The dendrogram investigation, principle component analysis, and correlation study were discussed and interpreted according to geography, geology, hydrogeology, and anthropogenic sources.

Key words: Hydrogeology, hydrogeochemistry, modeling, northern Sinai.

INTRODUCTION

In arid and semiarid regions, recharge fluxes are often very small percentage of the total precipitation falling over the basin and highly heterogeneous in space and time (Wilson and Guan, 2004). The quality of groundwater is of equal importance in many arid and semiarid areas, where the impacts and chemical processes related to salinization often represent the single largest threat to freshwater resources (Williams, 2001b). A common mechanism of groundwater salinization in areas of freshwater pumping is induced migration of local naturally occurring brackish, saline groundwater or seawater (Jennifer et al., 2008). In areas susceptible to pumping-

induced salinization, a diffuse mixing layer of variable thickness separates fresh and brackish groundwater. When fresh water sections are pumped, the positions of nearby mixing zones are affected directly and, if pumping rates are high enough, saline water may even move into the well' capture zone, resulting in contamination (Richter and Kreidler, 1993).

The Sinai Peninsula occupies an area of about 61,000 Km². The study area is located in the northeastern part of Egypt (Figure 1). The importance of the Sinai is referred to its location, where it constitutes the eastern border of Egypt and the first defiance line. Therefore, it must be done what is called the population development which depends on the development, economy, education, agriculture...etc. The groundwater is the main source for agricultural, municipal, domestic and drinking purposes.

*Corresponding author. E-mail: mohamedkashouty@yahoo.com.

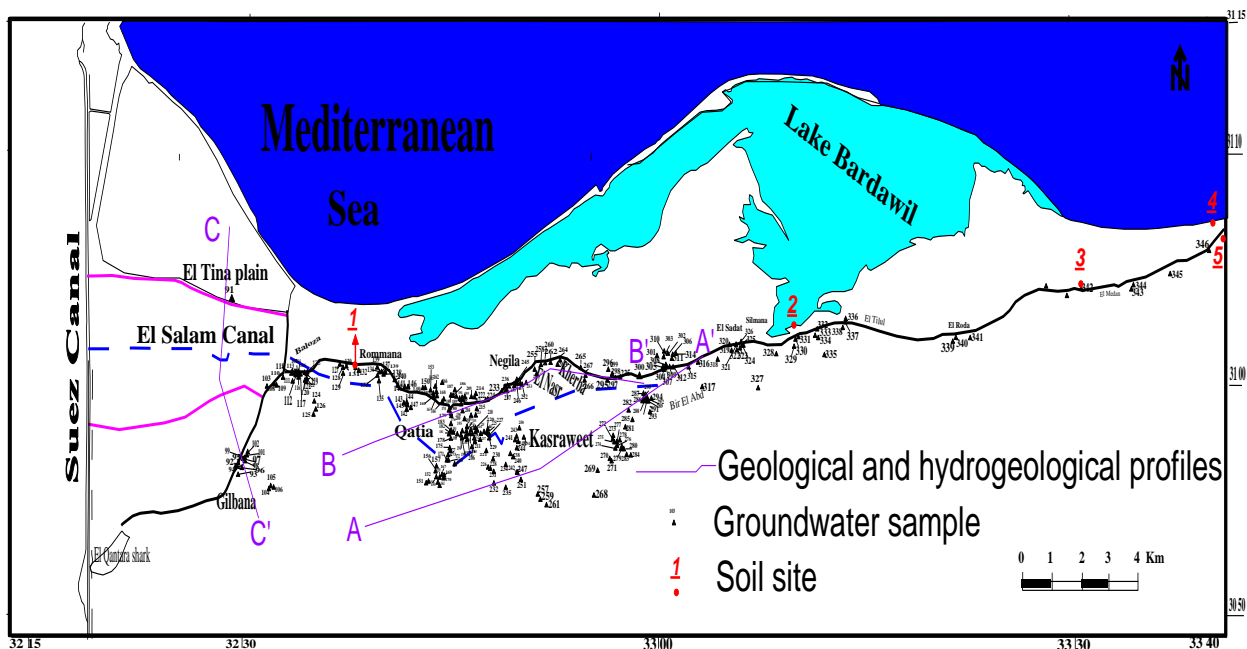


Figure 1. Location map of the northeastern part of Sinai Peninsula and the groundwater sample sites.

The expansion of the economy of Sinai, beside the rapid growth of its population in the last decade, has increased the water demands. The groundwater supply in the Sinai Peninsula is generally insufficient to meet the predicted increase in water demands. Accordingly, serious strategies for water development have been established to fully utilize the surface and groundwater resources at economic costs. Recently, the Sinai Peninsula has received great attention in respect to future agricultural development, especially after initiation of El Salam canal to the northern coastal area, as a source of irrigation. Therefore, a detailed groundwater investigation was undertaken to elucidate the principal hydrogeological and hydrogeochemical aspects of the northeastern part of Sinai. The average annual rainfall is about 83.36 mm at El Arish. The average temperature is 26.8°C in summer, while in winter is 14.6°C. Evaporation plays a principal role in the groundwater regime; they affect both the groundwater quantity and quality. The maximum mean monthly evaporation is about 17.4 mm/day in June [at El Maghara], while it is 5.2 mm/d in September [at El Arish] (El Said, 1994). The total evaporation decreases generally in the northeastern direction, i.e. towards El Arish and Rafah, while it increases due El Qantara –El Massaid (the investigated area about 100 mm/y).

MATERIALS AND METHODS

A 256 groundwater samples were collected from the Quaternary aquifer in summer 2008 period. The samples were numbered from 91 to 246 in the map site (Figure 1). The samples were acidified

with ultra pure nitric acid, after filtration, to avoid complexation and adsorption. The acidification was accomplished in situ and in case of heavy metals determination. Then the samples were transported to laboratory and stored at refrigerator at approximately – 20°C to prevent change in volume due to evaporation. The pH, temperature, and electrical conductivity (EC) are determined in situ. Ca^{2+} , Mg^{2+} , HCO_3^- , and Cl^- are measured titrimetrically. Na^+ and K^+ are estimated by flame photometer. SO_4^{2-} is established by the turbidity method. SiO_2 , B^{3+} , PO_4^{3-} , and NO_3^- are measured colorimetrically using UV/visible spectrophotometer, Unicam; model UV4-200. Br^- and I^- are determined potentiometrically by means of ion analyzer (ion-selective electrode) using ion-selective electrode, Orion Research Incorporation, model 940. Pb^{2+} , Fe^{3+} , Cd^{2+} , Ni^{2+} , Cu^{2+} , Zn^{2+} , and Co^{2+} are measured by Atomic Absorption Spectrophotometer, Unicam model Solaar 929. The analyses were carried out at the Desert Research Institute. The SPSS version 8 is used to discriminate the groundwater groups. Three pumping tests were performed to determine the hydraulic characteristics of the Quaternary aquifer. The infiltration tests were accomplished in five soil sites to determine the infiltration rate. The infiltration test is carried out using the double ring infiltrometer as described by (Black 1973). The five soil samples were collected within 0, 50 and 100 cm depth, fifteen soil sub samples were analyzed for grain size.

RESULTS AND DISCUSSION

Hydrogeology

The aquifer system

The Quaternary aquifer (Holocene and Pleistocene) thickness varies from 150 m (Bir El Abd well) to 330 m (Qatia-1 well) and rests directly on the Pliocene clay (A-A' profile, Figure 2), (El Osta, 2000). According to Abd El Aal (1992), El Said (1994), and El Osta (2000), the

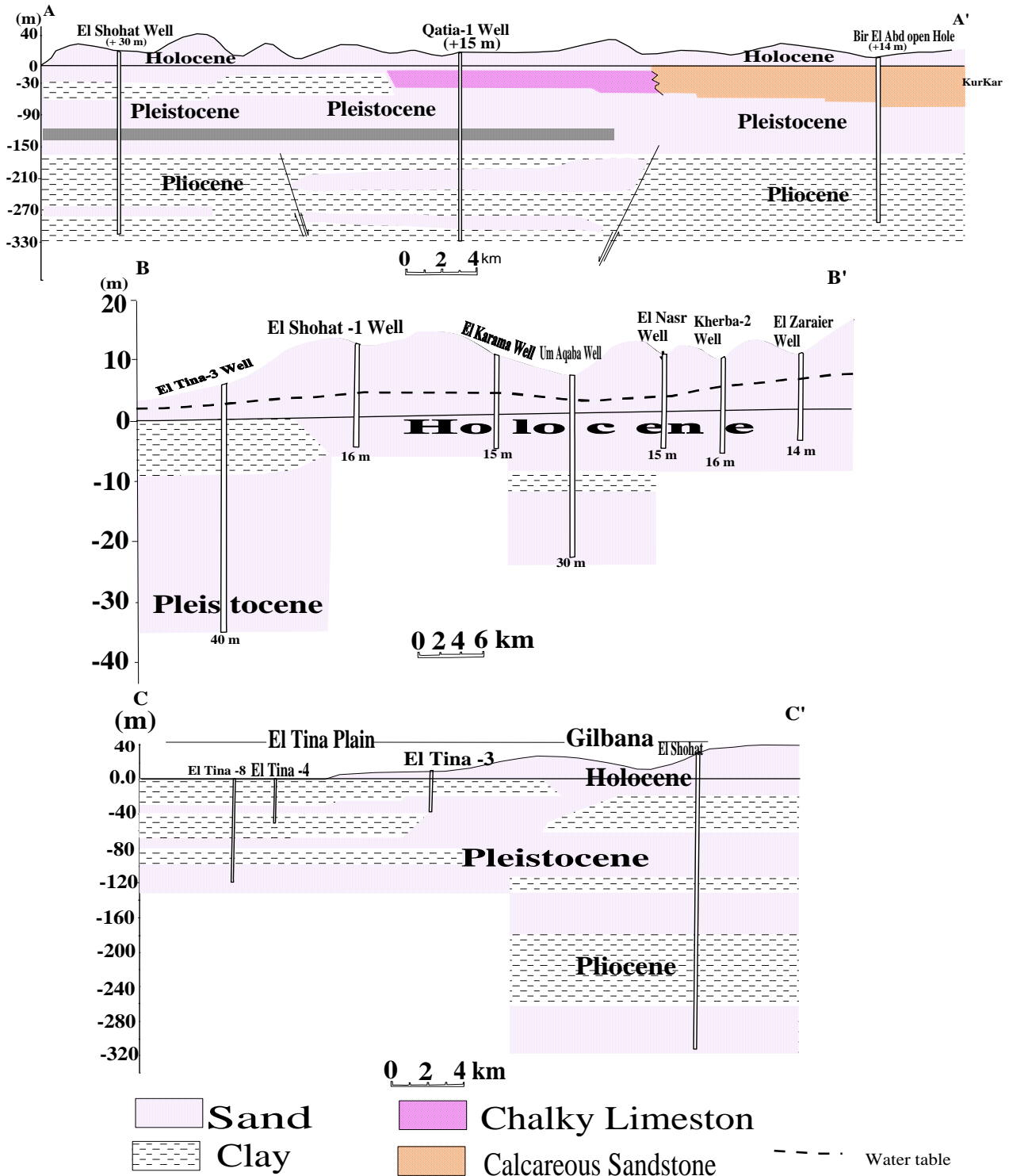


Figure 2. Geological and hydrogeological cross sections (shown in Figure 1) in northern Sinai.

groundwater in the southern Lake Bardawil (northern Sinai) is tapped from different water bearing formations, which are Holocene and Pleistocene. The Holocene sand aquifer in the studied area is developed along the coastal plain from Gilbana to El Massaid along a distance of

about 150 km with average width 20 km in the form of elongated sand dunes (coastal) or sand sheet (inland) or saline sand (sabkhas). On the other hand, this aquifer wedges out at El Tina plain until it vanishes. The loose sand is essentially composed of quartz grains coated with

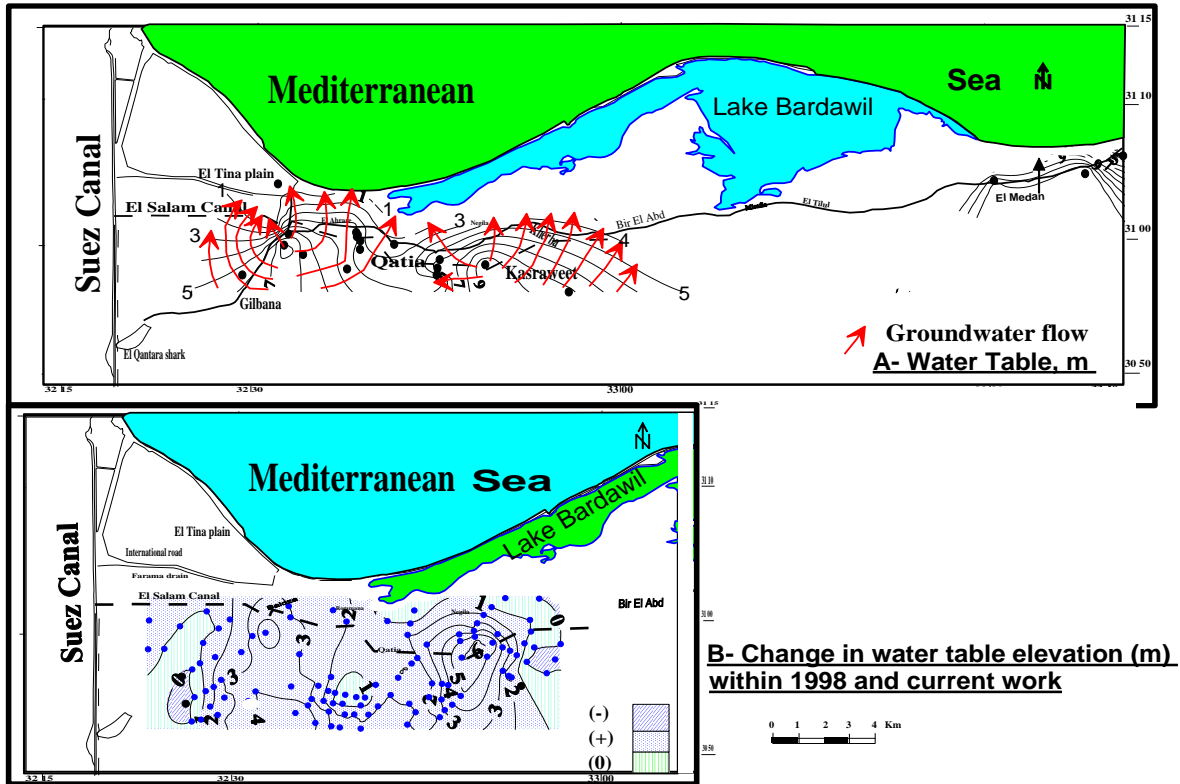


Figure 3. Water table elevation (A) and change within 1998 and current work (B) in the Quaternary aquifer in northern Sinai.

iron oxides mixed with few carbonate material. The groundwater of the Holocene aquifer exists under free water table condition, where depth to water ranges from 2 to 9.92 m below ground surface. However, this depth is very near to the ground surface close to the sea shore (B-B' profile, Figure 2). The infiltration and percolation from direct rainfall and surface runoff is the main source of recharge in the aquifer. The alluvium aquifer (Pleistocene) is commonly composed of sands and gravels with intrusion of silt and clay. Due to the capability of the alluvial deposits to store and transmit groundwater, the alluvium aquifer represents one of the most productive aquifers in the studied area. Rainfall intensity greatly affects the rate of recharge of such aquifer. In El Tina plain, the groundwater comes very near to the ground surface. The depth to water varies from less than one meter at north to about 2 m at south as a result of the presence of cap rock (30 m clay), where such aquifer in El Tina plain area is confined (C-C' profile, Figure 2) (El Osta, 2000). To the southern part of El Tina Plain (East El Qantara), the Pleistocene aquifer is about 170 m thickness and it rests directly on the Pliocene aquiclude, where both the Holocene and Pleistocene aquifers are partially hydrogeologically interconnected (C-C' profile, Figure 2) (El Osta, 2000). On other hand, in Qatia area, the Pleistocene aquifer

attains about 300 m in thickness due to presence of graben structure.

The water table

The water table level of the Quaternary aquifer ranges between less than 2 m at El Tina plain to +12 m at the coastal area at El Medan. The regional groundwater flow is directed towards north, locally towards NW (El Tina Plain) and northeast (Figure 3A), where the recharge area is the mountains of Gabel El Maghara, which lie in southern part of the study area. The overlap of water table in 1998 and present work yield change in water table map (Figure 3B), which reflect the following:

1. Areas of rising water table level, (+1 to +6 m), are around El Salam canal (Baloza, El Ahrar, Qatia, Kasraweet, El Nasr and Kherba) (Figure 3B). The rate of recharge exceeds that of the discharge;
2. Areas of groundwater depletion (over-pumping zone), (-1 m) at southern El Qantara and El Kasraweet. They referred to water extraction more than the water recharge; and
3. Areas of constant water level are in Kherba, Negila and Gilbina, where the withdrawals are nearly equal to

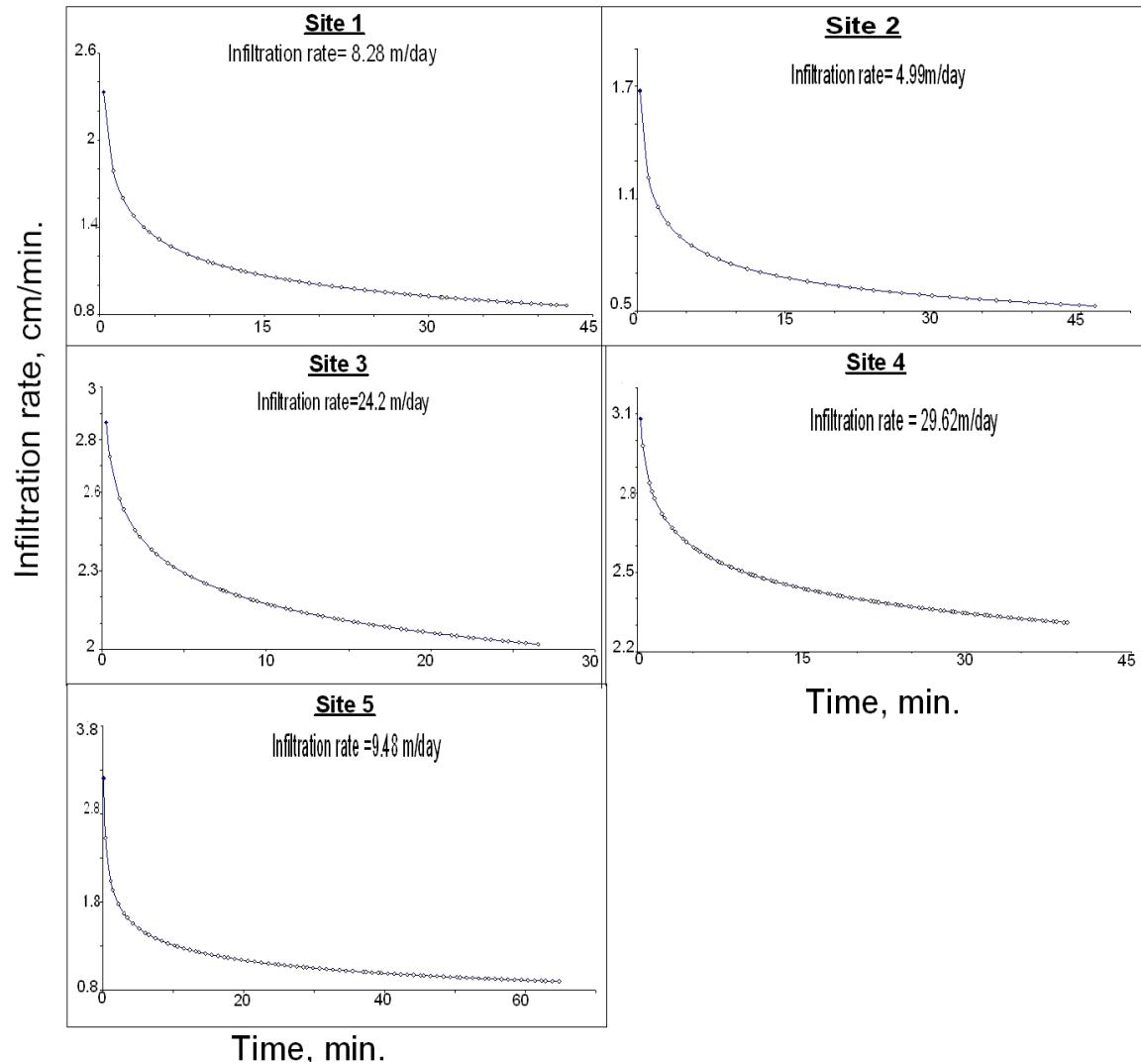


Figure 4. Infiltration test curves of the five soils in northern Sinai.

the recharge.

Infiltration rate and granulometric analysis

For all the studied soil types, the slope predicted from the obtained cumulative infiltration curves is less than unity and more than zero. For convenience, the slope of the obtained curves is suggested a high infiltration rate at the beginning of infiltration test due to the large hydraulic gradient between groundwater and soil-bounded water (unsaturated flow) (Figure 4). Afterwards, it decreases with time until it reaches a constant value (basic infiltration capacity or a soil parameter related to (K_{sat}) (Figure 4). According to grain size analysis of dry soils (Figure 5) and infiltration rate classification (Kohnke, 1980), it can be concluded that the infiltration rate at Misafiya area is rapid infiltration rate 4.99 m/day (test 2). This area is composed of medium to fine sandy textured soil. The

soils at coastal area (Rommana, soil 1), El Medan (soil 3) and El Massaid (soils 4 and 5) are characterized by very rapid infiltration rate 8.28, 24.2, 29.62 and 9.49 m/day, respectively. These localities are mainly composed of medium sized sand.

Transmissivity and storage coefficient

For determining the hydraulic parameters of the Quaternary aquifer in the study area, two pumping tests were accomplished for two hand dug and drilled wells in October (2008). The drilled well is partially penetrated the aquifer to depth (21-30 m), while the hand dug well is only penetrated the shallow zone of the Quaternary aquifer. The third pumping test was reanalyzed data of El Masharif drilled well after (Abd El Aal, 1992). The first pumping test data of Rommana hand dug well (site 2) is illustrated using Papadopoulos and Cooper (1957) method

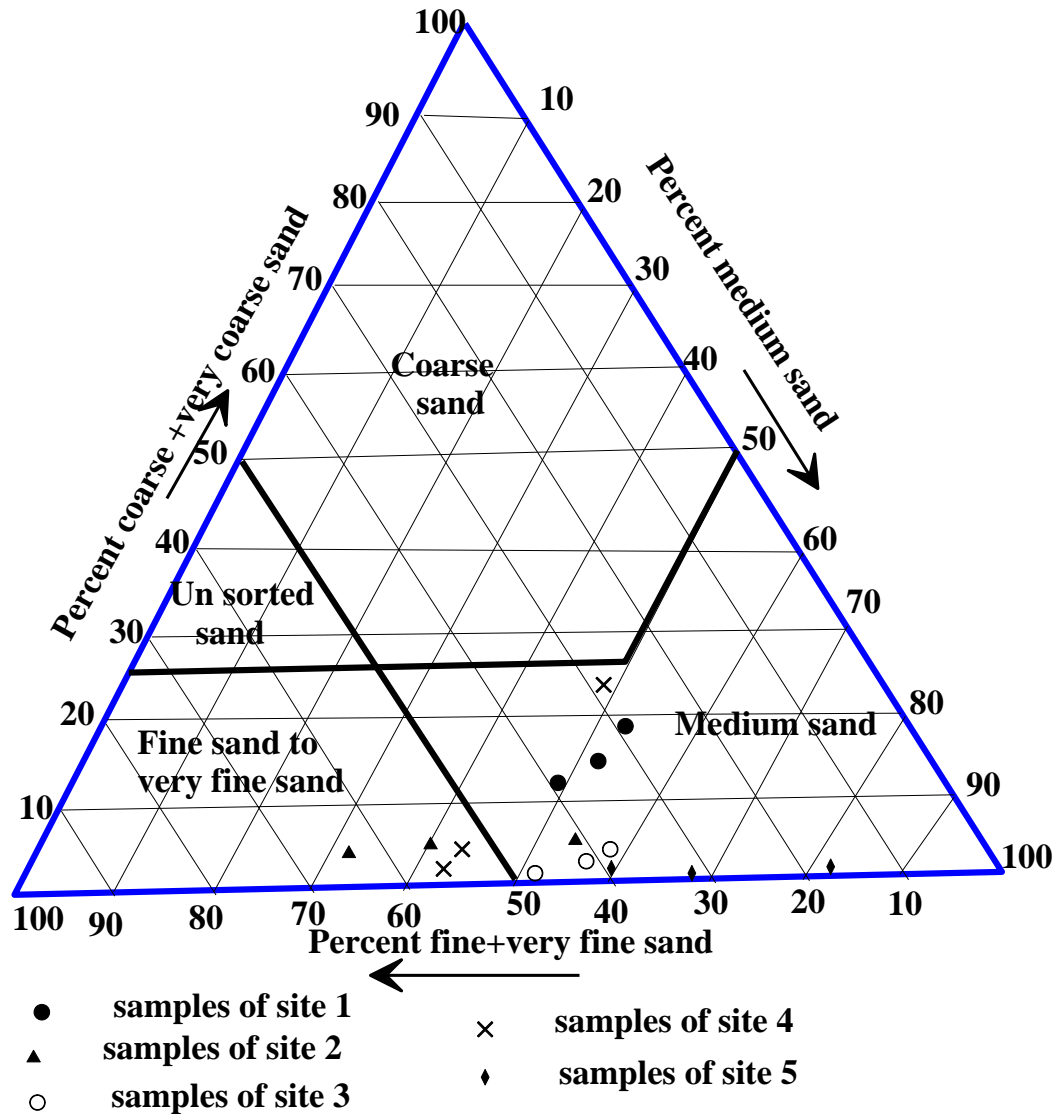


Figure 5. Triangular diagram sand subclasses of the fifteen sub soils in northern Sinai.

(Figure 6). The transmissivity (T) and storage coefficient (S) are calculated from the following equations:

$$T = rw^2S/4tuw \text{ and } S = \alpha rc^2/rw^2$$

rw: is the radius of pumped well (m); rc: radius of the well casing; S: The dimensionless coefficient of storage; T: The transmissivity of the aquifer (m²/day); t: is the time value for matching point on the time-axis (day); F(uw, α): is the well function in uw and α.

The value of the transmissivity (T) and storage coefficient (S) are 112.75 m²/day and 1.16×10⁻³ respectively. The second pumping test data of El Tina drilled well is constructed using Theis method (Figure 7A). T and S parameters can be calculated applying the following relations (Theis, 1935):

$$T = QW(u)/4\pi s \text{ and } S = 4Ttu/r^2$$

W(u) and U: well functions; U=r²S/4Tt; s: The drawdown (m) measured in a piezometer at a distance r (m) from the pumped well; Q: The constant well discharge (m³/day); S: The dimensionless storage coefficient; T: The transmissivity of the aquifer (m²/day); t: The time since pumping started (day).

The transmissivity (T) and storage coefficient (S) of the Quaternary aquifer in El Tina drilled well are 84.80 m²/day and 9.4×10⁻⁵ respectively. The third pumping test at El Masharif drilled well was shown in Figure 7B. The aquifer transmissivity and storativity are 294.47 m²/d and 1.61 * 10⁻², respectively. The Quaternary aquifer has moderate potentiality, (transmissivity ranges from 50 to 500 m²/d) according to (Georhage, 1979) classification in

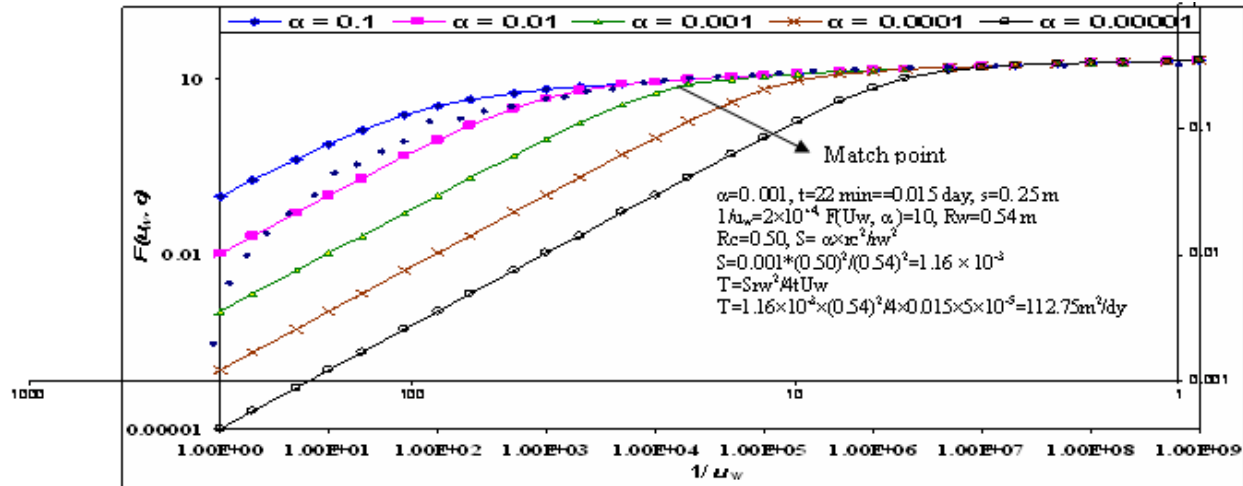


Figure 6. Recovery data analysis of Rommana hand dug.

three investigated pumping tests. The Quaternary aquifer is high potentiality ($T > 500 \text{ m}^2/\text{d}$) in the four left wells in Figure 8, while the rest wells are moderate potentiality. The storativity at El Tina plain is reflected a confined type, while the other two investigated wells are indicating phreatic and semi confined. The collected wells in Figure 8 contain the storage coefficient value which ranges from unconfined to semi confined to confined type.

Hydrogeochemistry

Total dissolved solids (TDS)

Based on the total dissolved solids (TDS) concentration, the area can be classified into three sub regions (A, B and C). The TDS concentration in sub region (A) is increased due north (Figure 9A). It reflects the impact of seawater intrusion. The reverse trend is noticed around El Salam canal (sub area B), the TDS concentration is increased in the southern part. It is caused by dilution from El Salam canal. The exception for sub area B was noticed at Qatia and Gilbana. At Qatia, the TDS concentration is increased due north (Figure 9A). This is attributed to presence of Holocene aquifer underlain by chalky limestone (Figure 2). At Gilbana, the TDS concentration is increased towards the southwestern part due to recharge from El Qantara canal (saline water). On the other hand, the TDS concentration is increased in the northwestern direction, i.e. towards the Sues canal in sub area C, which is caused by seawater intrusion of Suez canal.

The TDS concentration of the Quaternary aquifer is controlled by the amount of rainfall, sea water intrusion, seepage from El Salam canal and the over exploitation activity. Nevertheless, salts evaporates, lithogenic source, and evaporation process play an important role in

the groundwater salinity particularly at the shallow depths. The difference between TDS concentration in 2000 and present work is estimated in a map (Figure 9B) and interpreted as follows:

1. TDS concentration increase areas are in the southern Qatia and El Tina plain. The water extraction exceeds recharge; which causes seawater intrusion;
2. TDS concentration decline areas are encountered around El Salam canal, where recharge exceeds the pumping. It is attributed to fresh water recharge from El Salam Canal;
3. TDS concentration constant are encountered at the southern El Salam canal, where the water extraction is more or less equal to recharge. The areas around El Salam canal shows decrease in TDS concentration and rise in water table. This gives good evidence for the seepage from El Salam canal.

Major ions

The distributions of Na^+ , Cl^- , SO_4^{2-} , Ca^{2+} , and Mg^{2+} concentrations are nearly similar (Figures 10A, B, C, D, and E). They follow, more or less, the pattern of TDS distribution map. They increased in concentration due northern part of sub area A, and in the southern part of sub area B. In sub area C they increased in concentration towards the northeastern direction. The HCO_3^- concentration follow TDS distribution map except sub area B (Figure 10F), which characterized by increase in HCO_3^- content due north. It is attributed to the recharge from El Salam canal. The higher concentration of Na^+ , Cl^- , SO_4^{2-} , Ca^{2+} , and Mg^{2+} is strictly confined to south of El Bardawil Lake. It is attributed to over pumping and influence of El El Bardawil Lake sabkhas. The average, ranges, and standard deviation were shown in (Table 1).

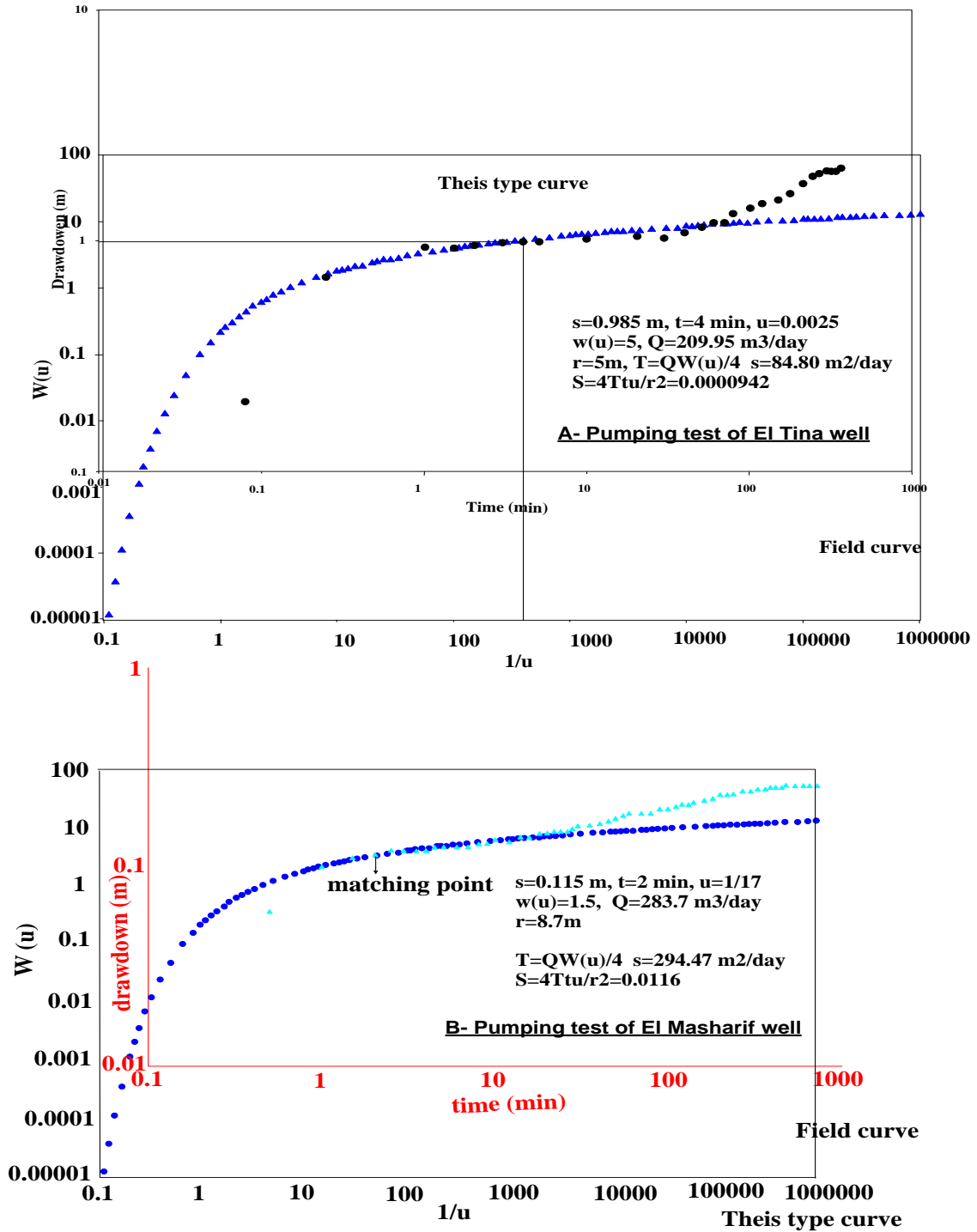


Figure 7. Pumping test data of El Tina and El Masharif drilled wells.

Minor and trace elements

Only 49% of water samples recorded boron concentration and the rest have concentration lower than detection limit (< 0.001 mg/L) (Figure 9C). B concentration increases in the northern part in sub area A, in the

southern part in sub area B, while in sub area C it is lower than detection limit (Figure 9C). The lower concentration of boron in sub area B and C reflect the dilution from El Salam canal, while in sub area A it caused by the effect of seawater. The concentration of NO³⁻ increased in the southern part of sub areas A and B

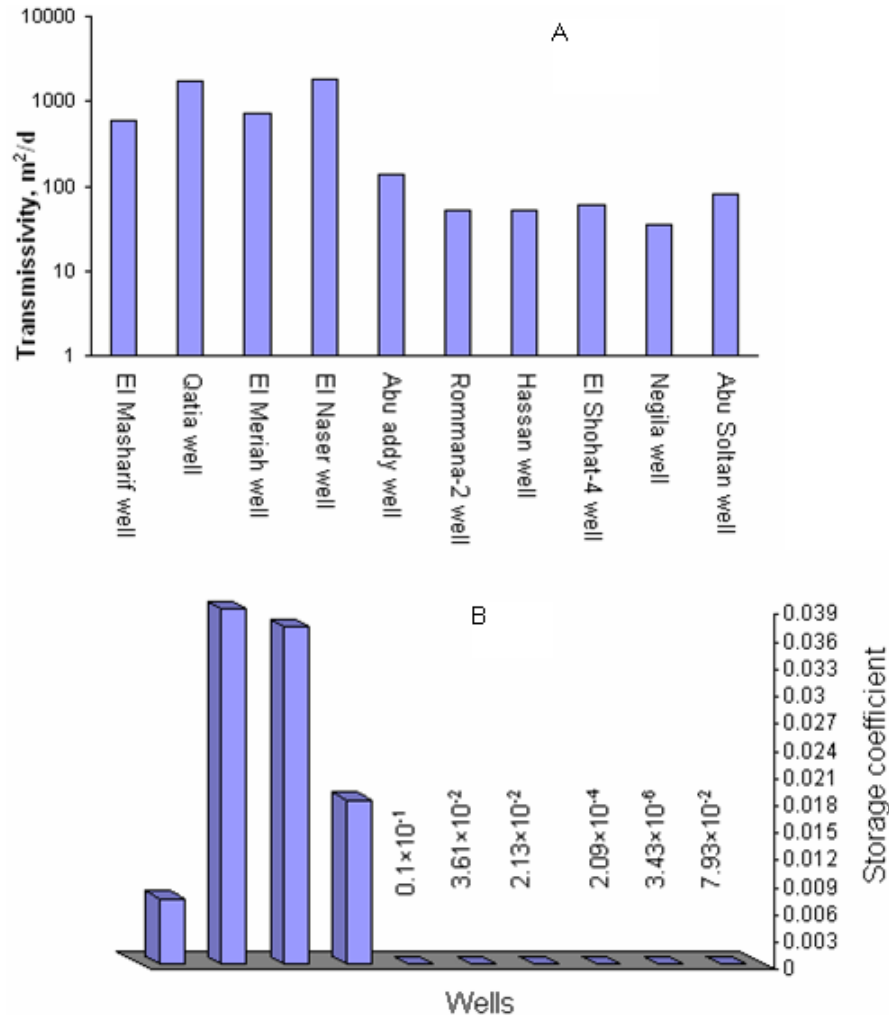


Figure 8. Collected transmissivity and storativity of the Quaternary aquifer in northern Sinai.

and in the southwestern part of sub area C (Figure 9D). The decrease in NO³⁻ concentration towards the Mediterranean Sea and Suez canal is caused by denitrification process and the source of nitrate seems to be related to agricultural activity. The NO³⁻ concentration at Qatia as mean is 50, which is lower than those in 2004 as mean 93 mg/L (El Alfy, 2004), it is due to dilution from El Salam canal. The source of phosphate minerals in Quaternary aquifer is due to over-use of phosphate fertilizers in irrigation where phosphate ions range from 0.12 to 2.08 mg/L with a mean value of 0.2 mg/L. In addition, this may indicate the effect of marine deposits, transported by weathering from catchment area to the aquifer matrices. The Br⁻ and I⁻ concentrations are generally low, they increases due northern part at Kasraweet village (sub area B), and northwestern direction at El Tina Plain (sub area C) (Figures 9E and 11A). This reflects the effect of seawater intrusion. Around El Salam canal (sub area B) Br⁻ and I⁻ concentrations are increased in the southern part. It is

caused by the dilution from El Salam canal. At Gilbana, Br and I concentrations are increased towards southeastern part, due to effect of Gilbana canal.

About 31% of groundwater samples are recorded Cu concentration while the rest are below detection limit (< 0.001 mg/L). It is generally low concentration, but it slightly increased in the northern part of Kasraweet village (sub area B) and in the northwestern part of El Tina Plain (sub area C). The Cu concentration not detected in sub area A (Figure 11B). The slightly increase of Cu concentration in sub area B and C is attributed to leakage from septic tank. The Mn concentration is increased at the center of the study area (sub area B). The Mn concentration is increased in the northern part of sub area B (Figure 11C). The domestic wastewaters and sewage may play important role for Mn concentration. The Cd concentration is increased towards southern and southwestern part in sub area B. At Negila, the Cd concentration is increased towards the northern part (Figure 11D). The Cd is related to agricultural activity in

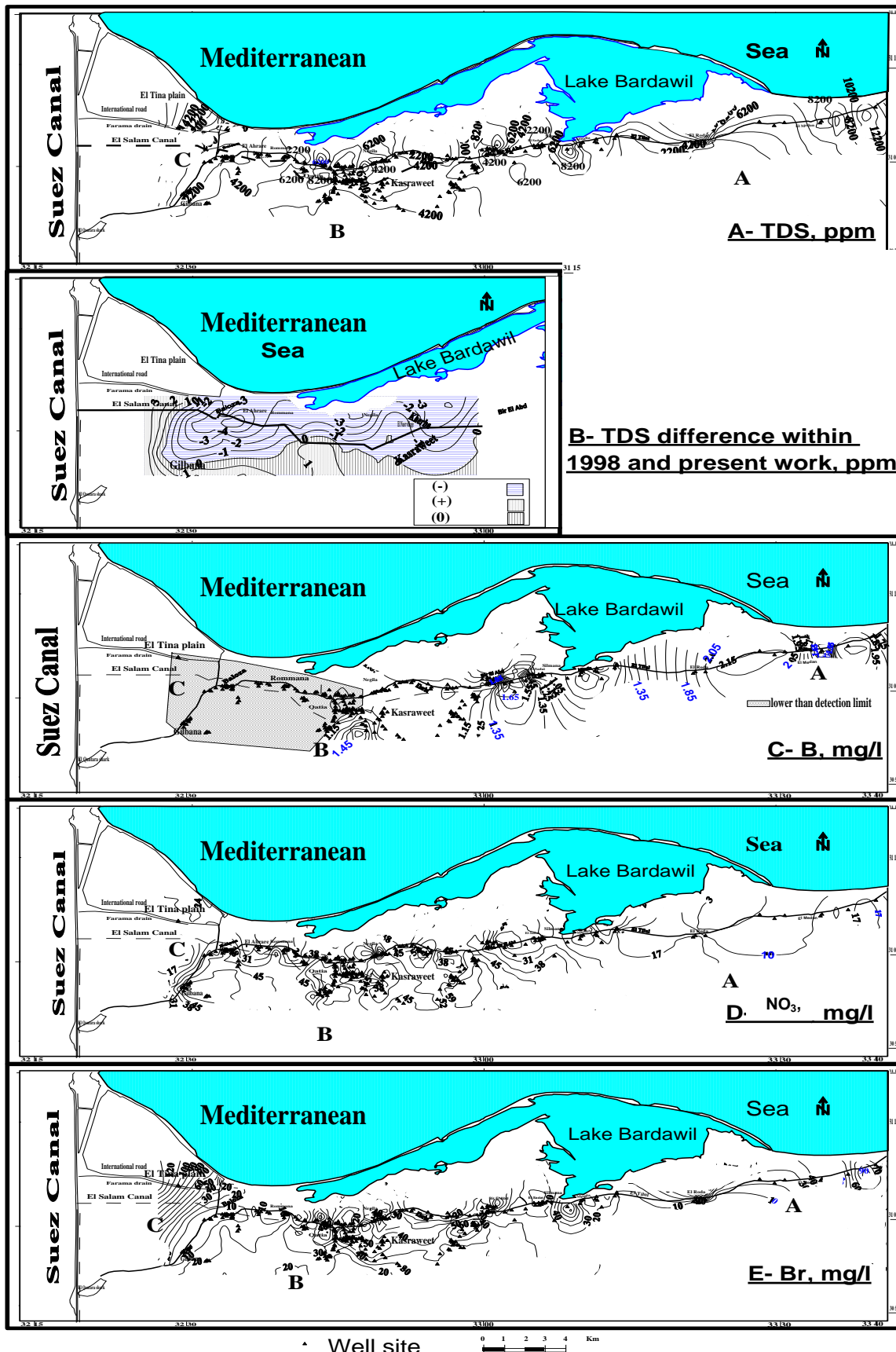


Figure 9. TDS, TDS change, B, NO₃, and Br concentrations in groundwater in northern Sinai.

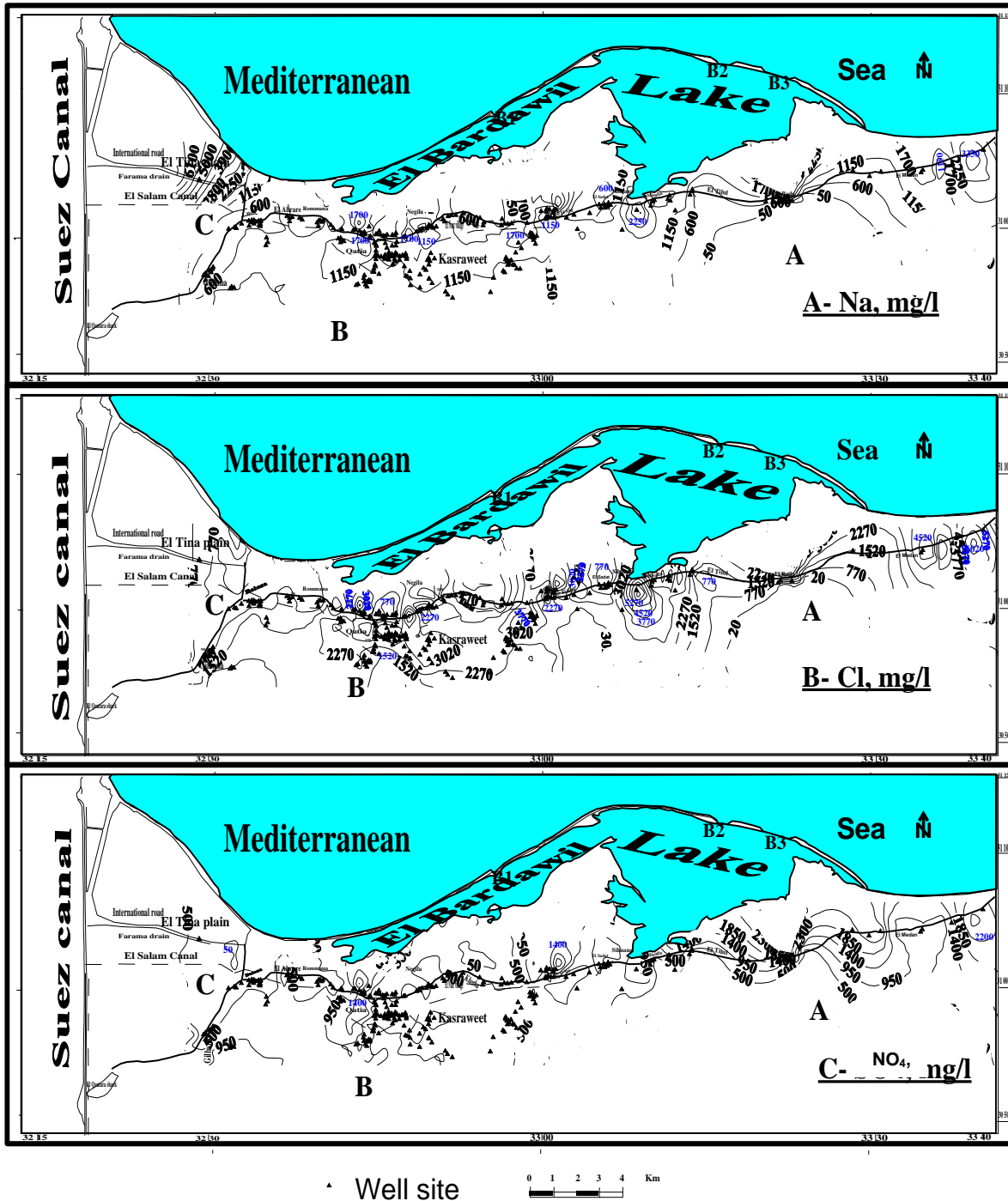


Figure 10. Na, Cl, SO₄, Ca, Mg, and HCO₃ concentrations in groundwater in northern Sinai.

sub area B, by application of phosphate and super phosphate fertilizers. The Fe concentration is increased towards the northern part of sub area B, northwestern direction of sub area C and southwestern part of Gilbana, (Figure 11E). The highest concentration of Fe was in sub area C and Gilbana, which caused by lithogenic and anthropogenic sources (leakage in sewer system). The

dilution from El salam canal causes a relative decrease in iron concentration in sub area B.

The Zn concentration is increased due the southern part in sub area A, and in the northern part in sub area B (Figure 12A). The highest Zn concentration was in Bir El Abd (14 mg/L). It is attributed to lack of sewer system. The Co and Ni concentrations are increased due the

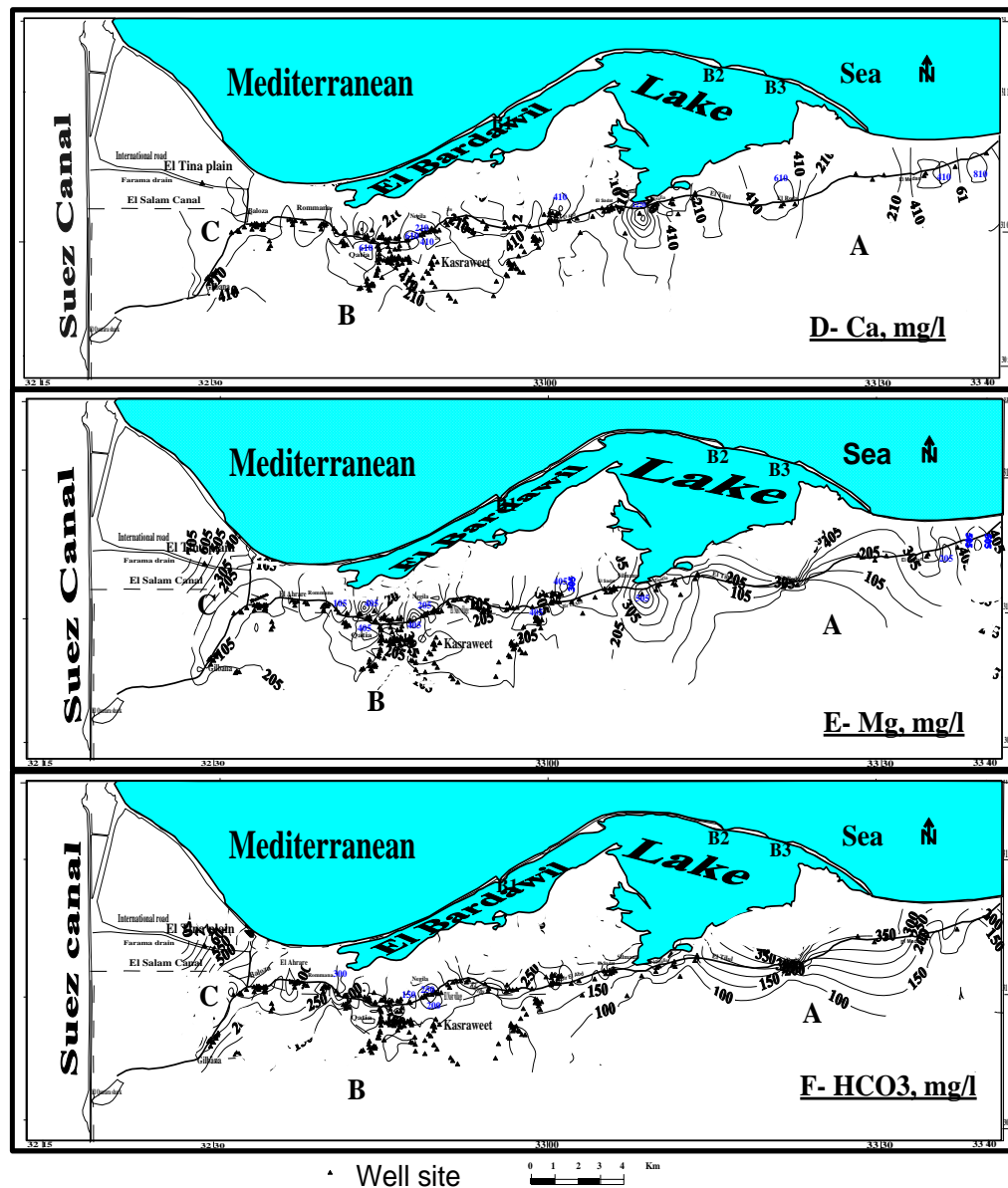


Figure 10. Cont'd.

Table 1. Min, max, mean, and standard deviations of major ions in groundwater in northern Sinai.

Element	Number of sample	Minimum	Maximum	Mean	Std. Deviation
EC	256	369	32600	7285.2	5292.3
PH	256	7.3	9.2	8.2	0.3
TDS	256	211.2	22761.7	4553.2	3498.5
Ca	256	8.2	1777.8	336.5	249.9
Mg	256	5	1039.5	214.4	168.6
Na	256	35	7200	1022.1	860.7
K	256	2	190	15.6	14.7
CO ₃	256	0	69.6	15.3	10.8
HCO ₃	256	61.9	734.1	183.6	94.9
SO ₄	256	30	4200	695.3	591.4
Cl	256	20	13359.9	2169.9	1854.6

northern part in sub area B (Figures 12B and 12C), which reflect the leakage of septic tank. In sub area A, the Co concentration is increased in the southern part. The Pb concentration is increased in sub area B, as result of leakage of septic tank (Figure 12D). It is noticed that, some of groundwater has concentration of trace metals higher than recommended limits in sub area B and C. This is attributed to leakage of septic tank in addition to effect of El Tina plain mud.

Multivariate statistical analyses

Hierarchical Cluster analysis (HCA) using Z scores

The raw data consisted of 18 hydrochemical variables (E.C., pH, TDS, Ca^{2+} , Mg^{2+} , Na^+ , K^+ , HCO_3^- , Cl^- , SO_4^{2-} , SiO_2 , B^{3+} , NO_3 , Fe^{3+} , Ni^{2+} , Co^{2+} , Br^- and I^-) of 162 groundwater samples, while the rest didn't statistically analyze because some heavy metals are below the detection limits. The cluster analysis helps in grouping cases into clusters on the basis of similarities within a cluster and dissimilarities between different clusters. The results of cluster analysis help in interpreting the data and indicate patterns (Vega et al., 1998). There are three clusters and one independent case (Figure 13). Cluster III include one sub cluster G which was represented by three cases. Sub cluster G is characterized by the highest average TDS concentration (17348 ppm), lowest average pH and HCO_3^- (4.64 and 103 ppm, respectively), and highest average Br (94.55 mg/l) concentrations. Sub cluster G is located at the coastal area, it is caused by seawater intrusion. Sub cluster G is characterized by high cobalt and iron concentrations. This is attributed to leaching and dissolution of the aquifer materials and leakage of septic tank. Cluster II classified into three sub clusters and six independent cases, sub cluster F included five cases. It is characterized by the TDS concentration lower than sub cluster G (average 11084 mg/l), the highest I and the high Br and NO_3 concentrations. It is due to the effect of seawater intrusion and agriculture wastewater. It is located at Negila in the coastal plain (Figure 14). Sub cluster F is characterized by the lowest cobalt, the low nickel and the high iron concentrations. The concentration of iron is caused by leaching and dissolution of Quaternary aquifer (lithogenic sources). Sub cluster E included four cases, it is characterized by medium salinity (average 6195 mg/l); lower than previous one, it has the highest average SiO_2 and lowest Fe concentrations. This is caused by leaching and dissolution process during the flow of groundwater. Sub cluster E is located along the coastal plain beside Lake Bardawil (Figure 14). Sub cluster D included three cases, which are characterized by high salinity (average 10959 mg/l), it is higher than the previous one and lower than sub cluster F. It is located near Bardawil sabkhas (Figure 14). Sub cluster D has the highest average Fe

(0.98 mg/l), higher nickel and cobalt concentrations than those in cluster F. The high concentrations of trace elements are related to anthropogenic sources (leakage of septic tank). Cluster II included six independent cases, well nos. 303, 317, 153, 130, 176 and 339. The independency is attributed to the highest nickel for well nos. 303 and 317, low Fe for well no. 153, lower NO_3 for well no. 130, high K for well no. 176 and highest SiO_2 concentrations for well no. 339. Cluster I is represented by three sub clusters and three independent cases, sub cluster C included ninety seven cases. It is characterized by medium salinity (average 5263 mg/l), lower than the previous sub clusters, it is caused partially by seawater intrusion and leaching and dissolution process. Sub cluster C is characterized by the highest concentration of NO_3 , resulted from agricultural fertilizers. It is in the southern El Salam canal where the rate of recharge from El Salam canal partially decline (Figure 14). The trace element concentrations of this cluster are relatively low. This reflects partially the effect of recharge from El Salam canal. Sub cluster B included six cases, it is characterized by the lowest salinity (average 663 mg/l), lowest average Br concentration (1.6 mg/l), this reflect the main source of recharge is the rain water. It is located at the eastern part of the study area where the rate of rainfall increases (90 mm/year) (El Osta, 2000). Sub cluster B is characterized by high iron, nickel and cobalt concentrations. The source of heavy metals is lithogenic rather than anthropogenic. Sub cluster A included thirty four cases. It is characterized by low salinity concentration (average 793 mg/l); which is higher than the previous one, highest average of HCO_3^- , lowest average of SiO_2 and lower average Br concentrations. This is caused by the dilution from El Salam canal. It is located around El Salam canal at the area affected by seepage of El Salam canal (Figure 14), as well as less leaching and dissolution processes. It is characterized by lowest cobalt and nickel concentrations due to dilution from El Salam canal. The independent cases of cluster I are due to the high value of HCO_3^- for well nos. 215 and 131, and lower Na concentration for well no. 344. The independent case (well no. 91) is due to highest TDS, Br and Fe concentrations. The average and ranges of the sub clusters identified by HCA was shown in Table 2.

Principle component analysis

Factor analysis, which includes Principle Component Analysis (PCA), is applied to reduce the dimensionality of data set consisting of a large number of inter-related variables, while remaining as much as possible the variability present in data set. Principal components are the linear combinations of the original variables and the eigenvectors (Wunderlin et al., 2001). Varifactors (VFs), which are a new group of variables, are obtained by rotating the axis defined by PCA. Grouping of the studied

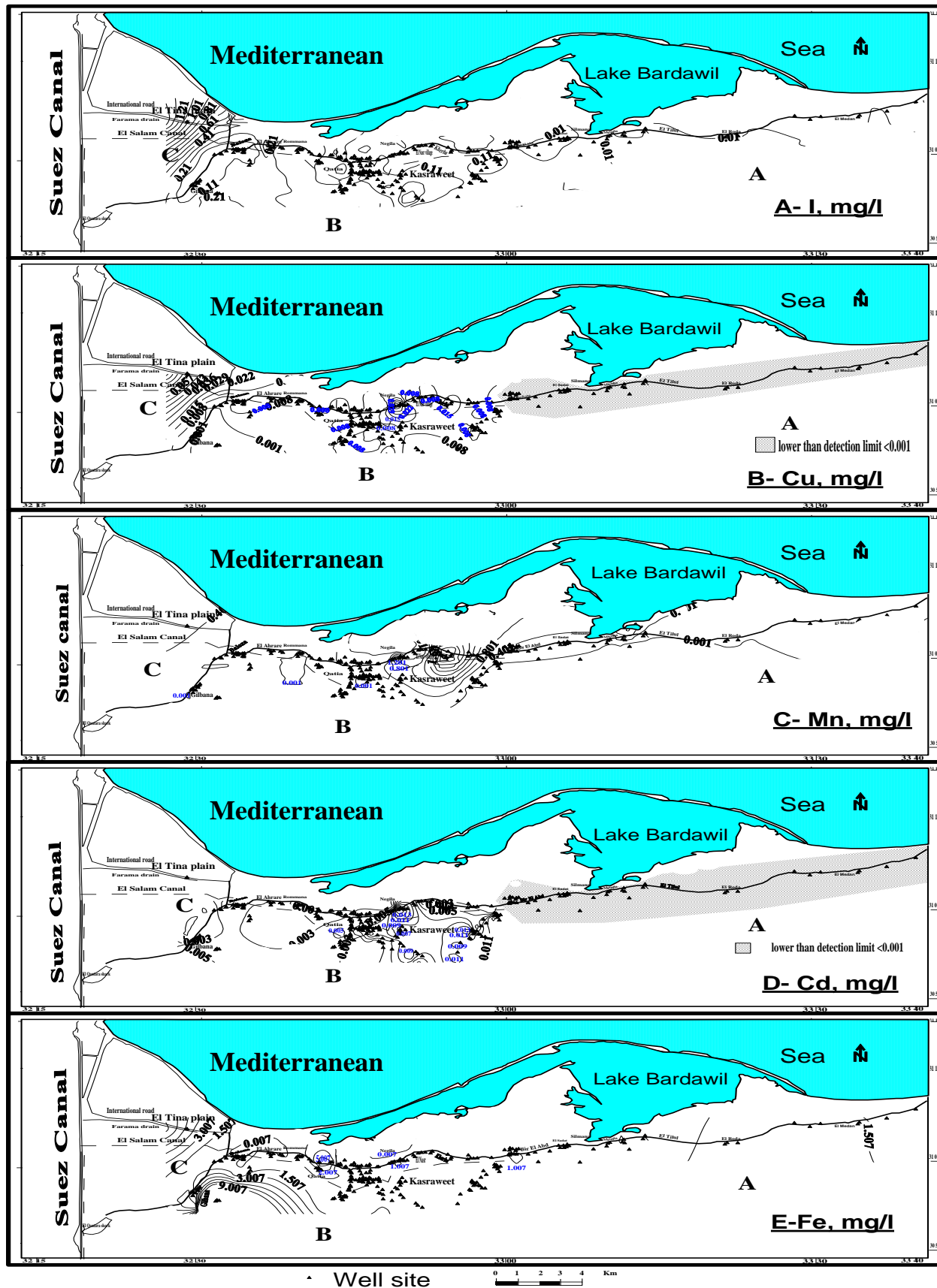


Figure 11. I, Cu, Mn, Cd, and Fe concentrations in groundwater in northern Sinai.

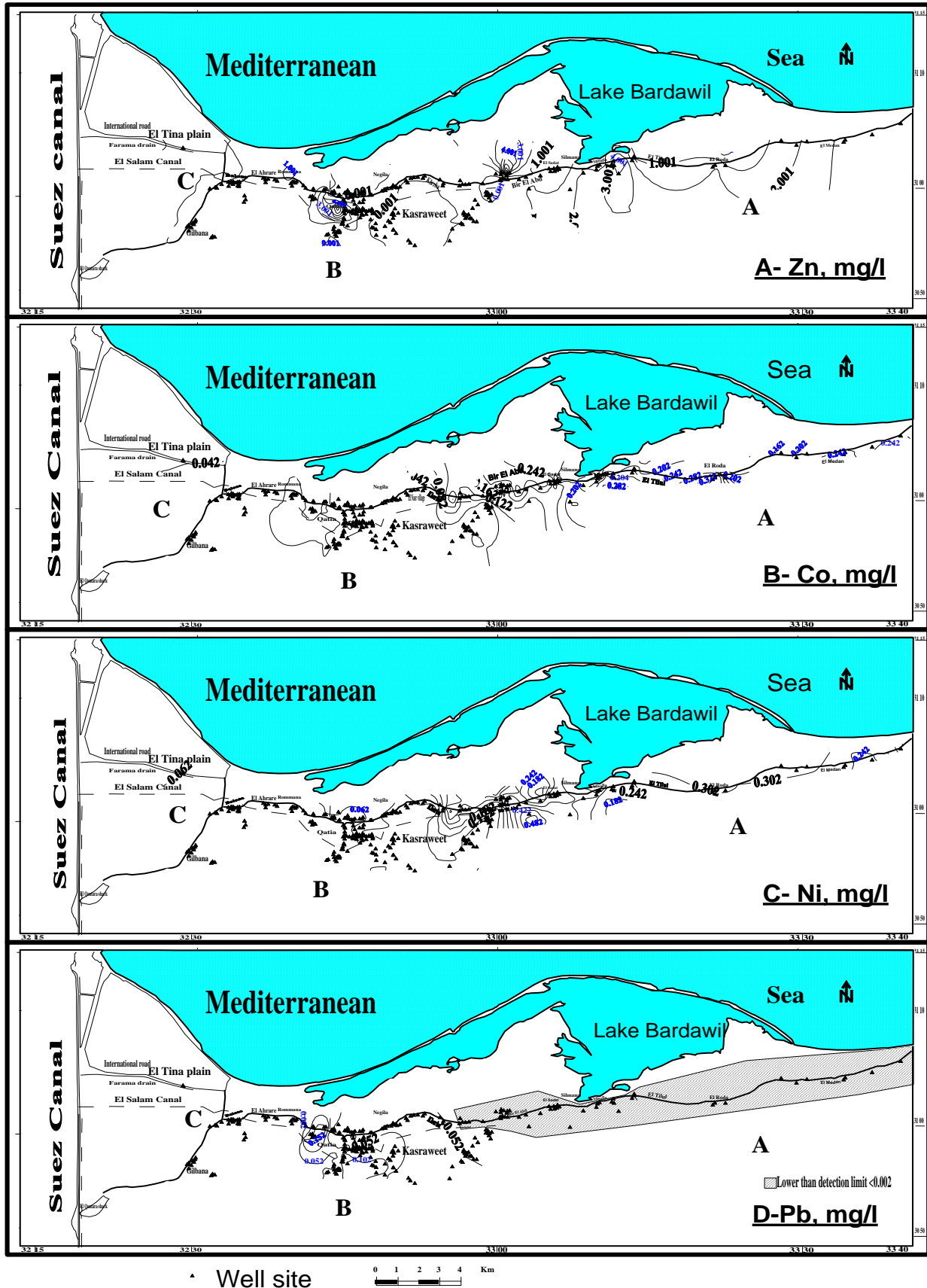


Figure 12. Zn, Co, Ni, and Pb concentrations in groundwater in northern Sinai.

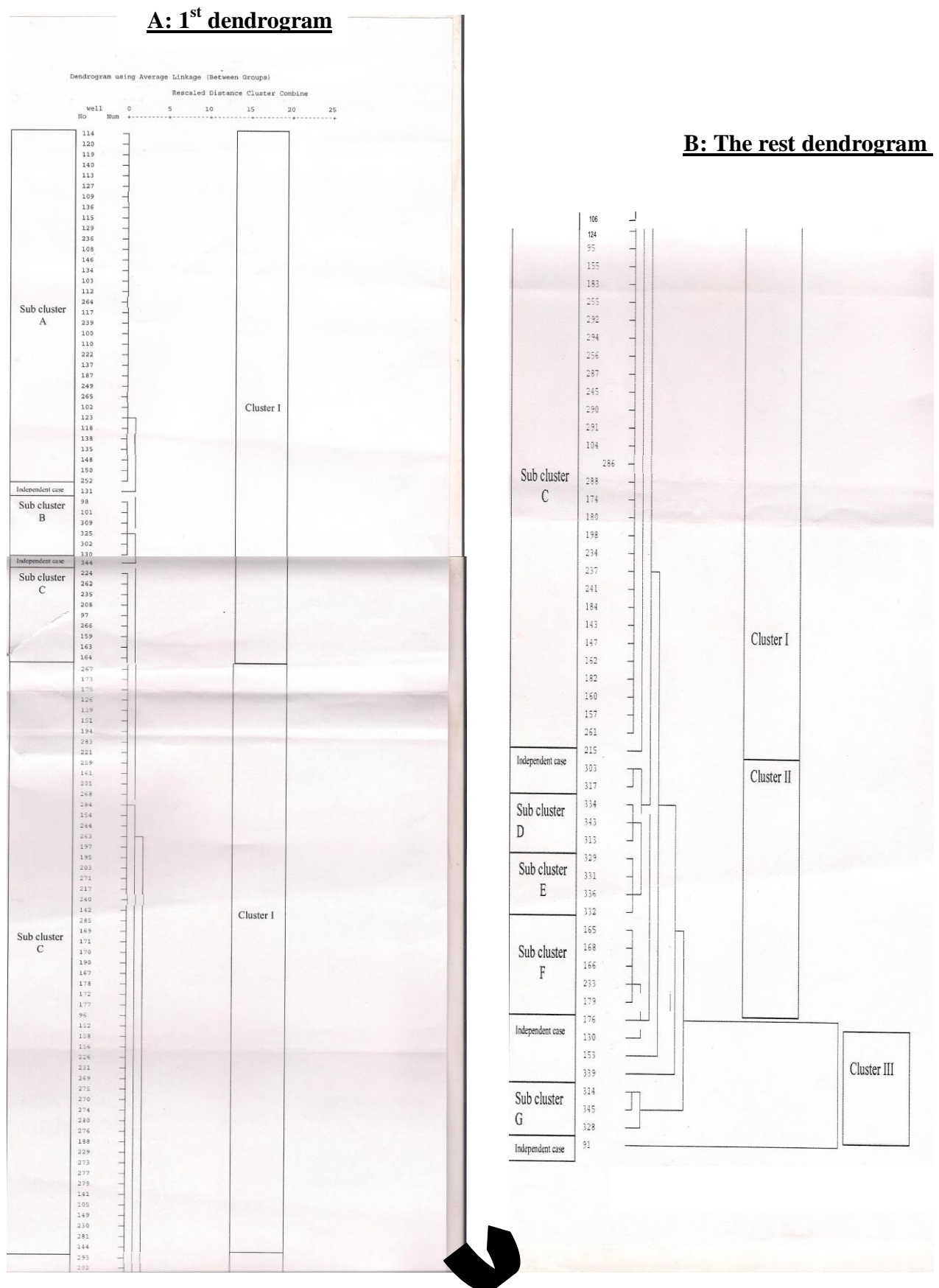


Figure 13. Dendrogram analysis of major and trace elements of the groundwater system in northern Sinai.

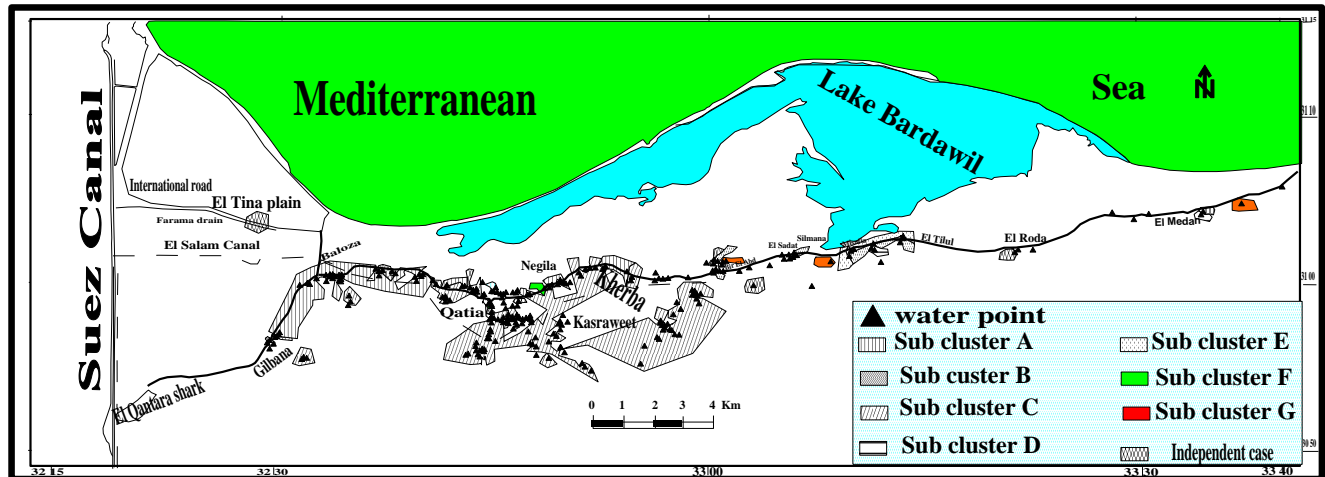


Figure 14. Areal distribution of sub clusters identified by HCA of Quaternary aquifer in northern Sinai.

variables according to their common features by VFs helps in data interpretation (Vega et al., 1998; Morales et al., 1999; Helena et al., 2000; Simeonov et al., 2003; Singh et al., 2004). Three rotated factors were extracted that enhance the TDS concentration. This factor is negatively loading with PH, resulted by seepage of El Salam canal. The second factor has positive loading with K, HCO₃, Fe and I. It indicates lithogenic and seepage from El Salam canal. The third factor is positive loading with Ni, Co and SiO₂, while is weakly negative loading with NO₃. It indicates lithogenic sources for Ni, Co and SiO₂ and anthropogenic sources for NO₃ (agriculture activity).

Correlation investigation

TDS is strongly correlated with Ca, Mg, Na, SO₄, Cl and Br. It is attributed to the effect of evaporation process and seawater intrusion. TDS is weakly correlated with K and I, the concentration of K is related to lithogenic source (leaching and dissolution of the Quaternary aquifer). The pH is negatively correlated with TDS, Ca, Mg, Na, Cl and Br and positively correlated with HCO₃. This indicate two sources of recharge, seawater for the former and fresh water (El Salam canal) for the latter correlation. The Ca is strongly correlated with Mg, Na, SO₄, Cl and Br. This is caused by seawater intrusion and dissolution of carbonate materials included in the aquifer sediments, which caused strong correlation between Ca and Mg. Ca is negatively correlated with HCO₃, attributed to dissolution of carbonate materials included in the aquifer that diluted from seepage from El Salam canal. The Mg is strongly correlated with Na, SO₄, Cl and Br, it is caused by evaporation process and seawater intrusion. The Na is strongly correlated with K, SO₄, Cl, I and Br, resulted from evaporation process, seawater intrusion

with total variance and Eigen values illustrated in (Figure 15). The first factor has positive loading with EC, TDS, Ca, Mg, Na, SO₄, Cl and Br. This reflects the seawater intrusion, evaporation, leaching and dissolution process and the lithogenic sources. The K is strongly correlated with I and is weakly correlated with Cl. The source of Cl and Br concentrations is evaporation and seawater intrusion while the source of K concentration is lithogenic sources. The SO₄ is strongly correlated with Cl and Br. It is attributed to the effect of evaporation process and seawater intrusion. The Cl is strongly correlated with Br and weakly with I. This is attributed to the effect of evaporation process and seawater intrusion. The Ni is strongly correlated with cobalt. This indicate that the source of Ni and Co concentrations is may be lithogenic. The Co is weakly correlated with SIO₂. The Co content is related to anthropogenic source (leakage of septic tank) and lithogenic source (leaching and dissolution of aquifer materials). The Br is correlated with I, related to evaporation and seawater intrusion.

Water quality

The TDS concentration (< 1000 ppm) is located separately around El Salam canal (Figure 16). These areas are suitable for drinking according to Egyptian standard (1995). The Cu and Zn concentrations are below the maximum contaminant level (MCL) for Egyptian drinking standard (1995) (1 and 5 mg/l, respectively). They also lower than the MCL for Egyptian irrigation standard (1995) (0.2 and 3 mg/l, respectively). The Mn content is exceeds the MCL for Egyptian drinking standard (1995) (0.05 mg/l) in the study are except the most southern part of sub areas B and C. The Cd concentration is higher than the MCL for Egyptian drinking and irrigation standards (1995) (0.005 and 0.01 mg/l,

Table 2. The average and ranges concentrations of major and trace elements of the sub clusters identified by HCA.

Cluster	Sub group	No.	Ec	PH	TDS	Ca	Mg	Na	
I	A	Range	520-2880	7.9-9.15	358.77-1627.09	8.16-224.48	4.95-92.98	45-380	
		Average	1266.71	8.62	792.94	54.74	38.72	182.93	
	B	Range	449-1850	8.33-8.72	244.73-1031	22.22-77.78	16.20-33.75	40-313.3	
		Average	1187	8.56	663.13	55.56	27.45	149.72	
	C	Range	2650-14500	7.29-8.62	1520.83-9655.97	81.63-734.69	74.38-520.71	250-2100	
		Average	8525.36	8.11	5262.97	418.79	252.63	1143.98	
	D	Range	16040	7.46-7.71	10148-11431.8	555.56-955.56	405-553	2350-3100	
		Average	17770	7.55	10959.1	777.78	463.5	2683.3	
	E	Range	6950-12260	7.84-8.05	3956-8023	267-722	243-459	850-1650	
		Average	9585	7.95	6194.92	477.78	362.81	1241.67	
II	F	Range	11300-19250	7.77-8.12	9145-13138.96	510-959	520.71-765.30	1600-2700	
		Average	15678	7.95	11084.12	820.4	646.49	2210	
III	G	Range	23700-25200	7.46-7.91	16258-18261	800-1777.78	540-810	3900-4600	
		Average	25533.33	4.64	17348.42	1192.59	2025	4166.67	
Cluster	Sub group	K	HCO ₃	SO ₄	Cl	Fe	Ni	Co	
I	A	Range	4--30	202.88-472.62	42.5-600	36.43-643.7	0.007-4.545	0.003-0.074	0.004-0.062
		Average	10.03	313.98	163.36	186.18	0.52	0.03	0.03
	B	Range	6--13	162.6-300.86	36-200	40-300	0.011-2.55	0.265-.53	0.089-0.26
		Average	8.67	246.65	132.67	158.75	0.89	0.33	0.18
II	C	Range	6--65	79.46-335.67	200-1700	388.65-5465.42	0.035-2.38	0.002-0.086	0.002-0.076
		Average	16.58	148.16	784.91	2572.01	0.37	0.04	0.03
III	D	Range	16-26	93.51-134.71	850-1000	5625-6250	0.467-1.636	0.25-0.371	0.174-0.246
		Average	20.67	108.42	916.67	6041.67	0.98	0.31	0.21
I	E	Range	17-42	142-182.95	300-1800	2187.5-1800	0.014-0.112	0.231-0.291	0.184-0.264
		Average	23.75	160.59	1050	2953	0.07	0.26	0.22
II	F	Range	17-24	70.76-203.43	1000-2600	3643.61-6072.69	0.171-2.15	0.01-0.084	0.007-0.058
		Average	19.6	118.52	2100	5222.49	0.85	0.05	0.03
III	G	Range	18-33	105.7-126	1700-4000	7500-10000	0.234-1.20	0.24-0.28	0.19-0.25
		Average	27.33	103	2900	8333.3	0.71	0.27	0.22
Cluster	Sub group	SiO ₂	NO ₃	Br	I				
I	A	Range	3--39	0-77.77	0.89-8.27	0.01-.10			
		Average	15.97	30.79	2.94	0.03			
	B	Range	3--33	6.45-49.66	0.39-2.72	0.0002-0.0006			
		Average	21.83	27.59	1.6	0.0004			
	C	Range	7--38	18.17-99.62	4.88-76.68	0.02-0.27			
		Average	21.96	49.69	35.98	0.11			

Table 2. Contd.

		Range	31-38	14.31-36.36	49.20-55.12	0.0068-0.1642
	D	Average	35	24.1	52.81	0.0613
		Range	33-63	9.42-38.84	14.88-34.51	0.0015-0.0955
II	E	Average	43	24.75	23.53	0.0266
		Range	19-22	20.79-52.9	40.41-85.6	0.17-0.30
	F	Average	20.6	31.85	70.41	0.235
		Range	22-47	6.87-22.2	84.78-102.14	0.019-0.023
III	G	Average	35.67	15.94	94.55	0.0215

respectively) in the northern part of sub area B. The Fe and Ni concentrations are exceeding the MCL for Egyptian drinking standard (1995) (0.3-1 and 0.02 mg/l, respectively). The Pb content is higher than the MCL for Egyptian drinking standard (1995) (0.05 mg/l) in sub area B. While it is lower than the MCL for Egyptian irrigation standard (1995) (5 mg/l). The B and NO₃ contents exceed the MCL for Egyptian drinking standard (1995) (1 and 10 mg/l, respectively). The B concentration exceeds the MCL for Egyptian irrigation standard (1995) (0.6 mg/l). Groundwater samples lie in the scale of 88 sample (Figure 17A). The most of the groundwater samples (46%) are good water for irrigation (C2-S1, C3-S1 and C4-S1), while about (38%) of the samples are moderate water for irrigation (C3-S2 and C4-S2). About 11% are intermediate water for irrigation (C3-S3 and C4-S3), and the rest are bad water for irrigation (C3-S4 and C4-S4) (Figure 17A). The most of groundwater samples are located in good to permissible class for irrigation (about 32%), while about 26% are located in doubtful to unsuitable class for irrigation. About 26% are located in permissible to doubtful class for irrigation. About (12%) of groundwater samples are located in excellent to good class for irrigation, and about three samples (4% of the represented samples) are located in the unsuitable class for irrigation (Figure 17B). This means that the

majority of the groundwater samples of the Quaternary aquifer (96%) are suitable for irrigation while the rest are unsuitable for irrigation.

Summary and recommendation

The present research is conducted to give an insight on the geochemical aspects of the Quaternary aquifer in northern Sinai, Egypt. The relationship between El Salam canal and the Quaternary aquifer are determined and evaluated through the assessment of groundwater quality. The aquifer system in the study area belongs to the Quaternary (Holocene and Pleistocene) age. The Holocene aquifer exists under free water table condition, where depth to water ranges from 2 to 9.92 m below ground surface. The Pleistocene alluvium aquifer is essentially composed of successive layers of water bearing sand separated by clay beds where these layers are hydraulically connected. The depth to water varies from less than one meter at north to about 2 m at south as a result of the presence of cap rock (30 m clay), where such aquifer in El Tina plain area is confined. The regional groundwater flow is directed towards north and locally towards NW (El Tina Plain). The infiltration rate at Misafiq area is rapid infiltration rate 4.99 m/day (soil 2). It is composed of medium to fine sandy textured soil.

The soils at coastal area {Rommana (test 1), El Medan (test 3) and El Massaid (tests 4 and 5)} localities are characterized by very rapid infiltration rate 8.28, 24.2, 29.62 and 9.49 m/day, respectively). They are mainly composed of medium size sand. The TDS concentration in sub area A is increased due north, reflect the impact of seawater intrusion, while in sub area B it is increased due southern part (around El Salam canal). It is due to dilution from El Salam canal. The TDS concentration is increased towards the southwestern part of Gilbina. The TDS concentration is increased towards the northwestern part of the Sues canal in sub area C, caused by sea water intrusion of Suez canal. The dendrogram analysis indicated three clusters, which subdivide into seven sub cluster depending on hydrogeochemical information of the Quaternary aquifer. The areal distribution of the sub clusters depended upon the geography of El Salam canal, seawater, lithogenic and anthropogenic impact. The Principal Component Analysis of the Quaternary aquifer is composed of three factors, which confirm the dendrogram investigation. The area around El Salam canal considered a promising area for exploration and exploitation of fresh water from the Quaternary aquifer, due to the hydrogeological interconnection between El Salam canal and the Quaternary aquifer. Management of the groundwater exploitation in

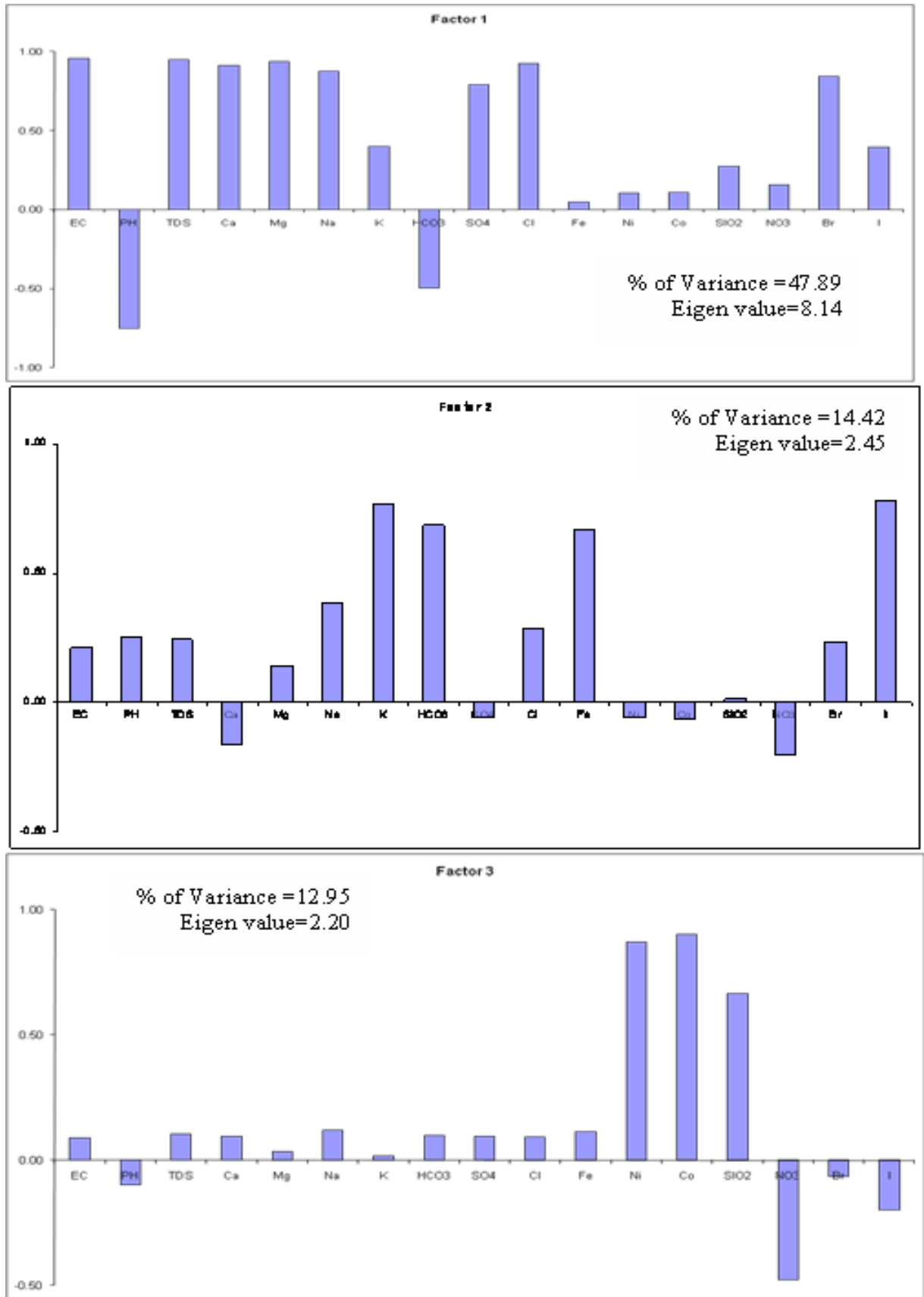


Figure 15. Factor analysis of the major and trace elements of the groundwater in northern Sinai.

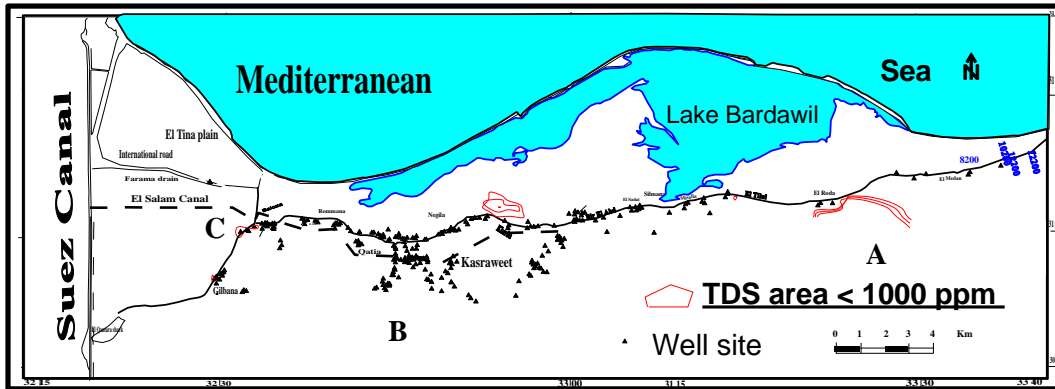


Figure 16. The TDS concentration (< 1000 ppm) distribution areas.

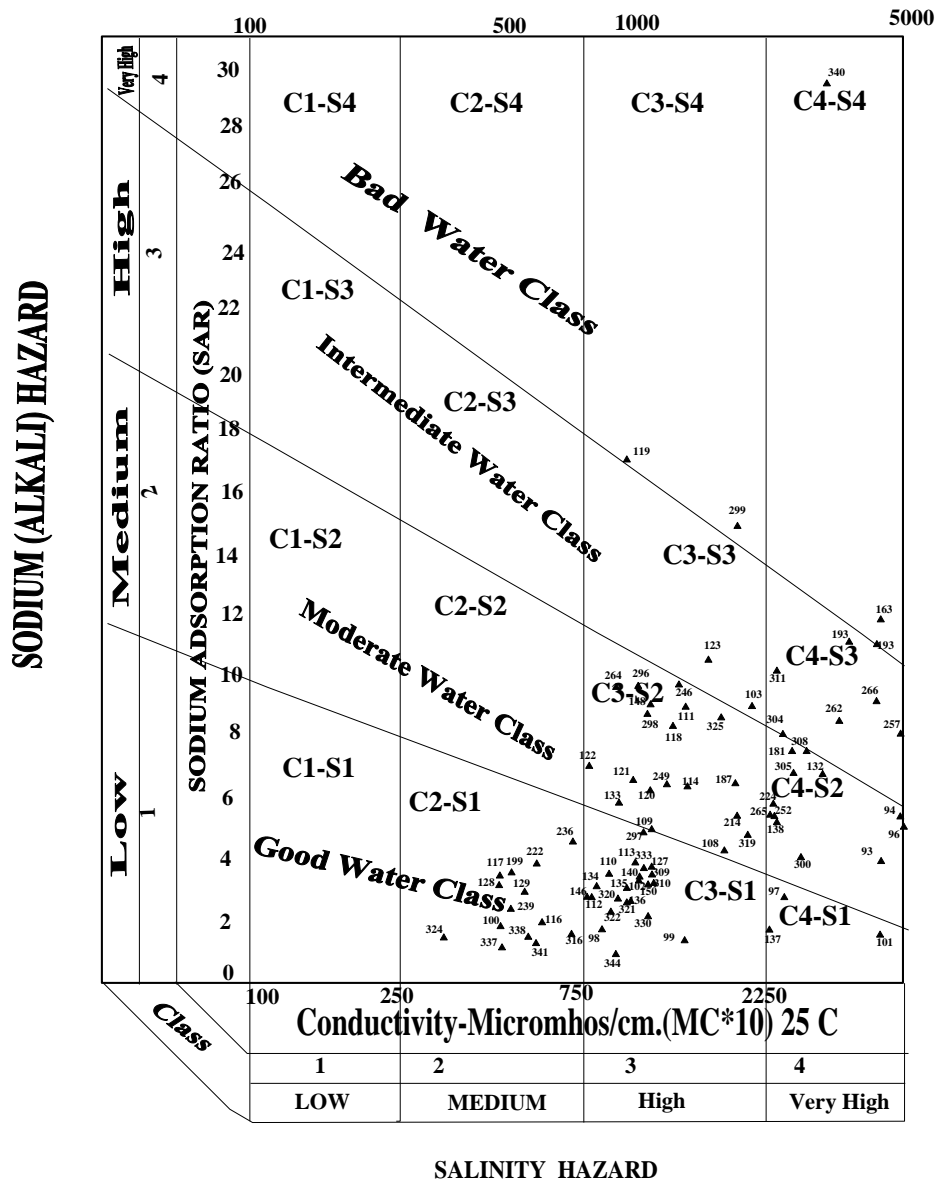


Figure 17A. The US salinity Staff (A) and Wilcox (B) diagrams for irrigation purpose.

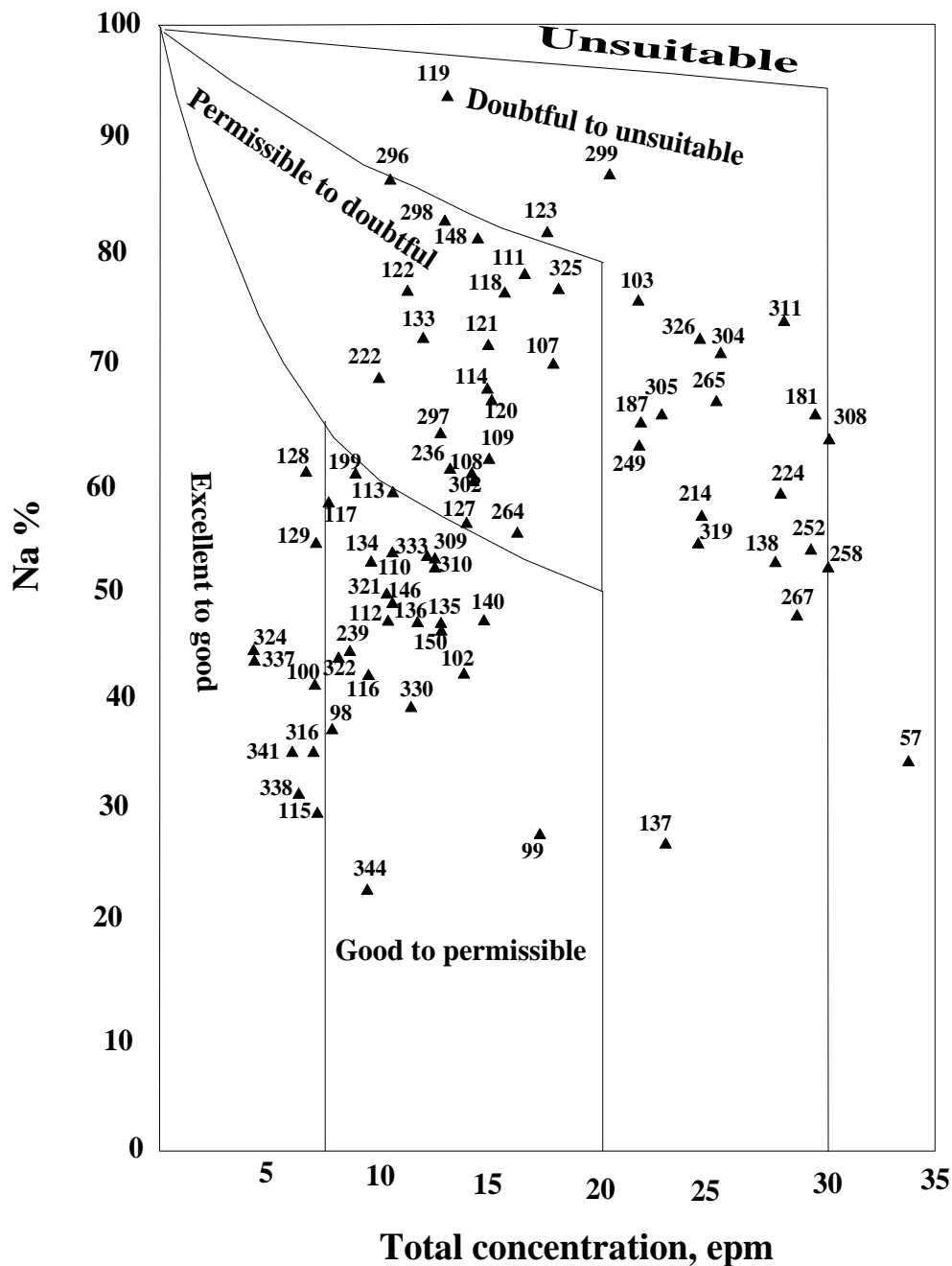


Figure 17B. The US salinity Staff (A) and Wilcox (B) diagrams for irrigation purpose.

the coastal aquifer must keep in mind to prevent pollution by the seawater, over-pumping, lithogenic and anthropogenic sources.

REFERENCES

- Abd El Aal G (1992). The ground water conditions in the area from Rommana to Bir El Abd, especially the area south of Rabaa Village, Northwestern Sinai Peninsula, A.R.E" M.Sc. Thesis, Geol. Dept., Fac. Sci., Cairo Univ., p. 145.
- Black C (1973). "Methods of soil Analysis". Am. Soc. Agron. Inc. Publ, Madison, 137 p.
- El Alfy M (2004). "Geochemical characteristics and pollution assessment of the groundwater of the Quaternary aquifer, Qatia area, north Sinai, Egypt" 6th intern. Conf. on geochemistry; Alex. Univ; Egypt. 15-16 sept.2004, pp. 271-292.
- El Osta M (2000). "Hydrological studies on the area between El Qantara and Bir El Abd,North Sinai, Egypt" M.sc. Thesis, Fac. Sci., Minufiya Univ., Cairo, Egypt.
- El Said M (1994). "Geochemistry of groundwater in the area between El Qantara and El Arish, North Sinai". Ph.D. Thesis, Fac. Sci., Ain Shams Univ., Cairo, Egypt.
- Georhage A (1979). "processing and synthesis of hydrogeological data."Abacus press, 290 pp.

- Helena R, Pardo M, Vega E, Barrado, Fernandez L (2000b). "Temporal evolution of groundwater composition in an alluvial – Pisuerga river, Spain by principal component analysis" *Water Res.*, 34: 807-816.
- Jennifer L, James H, Christopher E, Barry H, William H (2008). Hydrogeology controls on groundwater recharge and salinization: a geochemical analysis of the northern Hueco Bolson aquifer, Texas, USA. *Hydrogeol. J.*, 16: 281-296.
- Kohnke H (1968). "Soil Physical." Mc Graw-Hill Book Co., New York. 53 p.
- Morales M, Marti M, Liopis A, Campos L, Sagrado S (1999). "An environmental study by factor analysis of surface sea waters in the gulf of Valencia -Western Mediterranean" *Analytica chimica Acta*, 394:109-117.
- Papadopoulos I, Cooper H (1957). "Drawdown in a well of large diameter " *Water Resources Research Division. First Quarter, U.S.G.S.*, 3: 1.
- Richter B, Kreeitler C (1993). *Geochemical techniques for identifying sources of groundwater salinization*. CRC, Boca raton, FL, 258P.
- Simeonov V, Stratis J, Samara C, Zachariadis G, Voutsas D, Anthemidis A, Sofoniou M, Kouimtzis T (2003). "Assessment of the surface water quality in Northern Greece" *Water Res.*, 37: 4119-4124.
- Singh S, Malik A, Mohan D, Sinha S (2004). "Multivariate statistical techniques for the evaluation of spatial and temporal variations in water quality of Gomti River India- a case study " *Water Res.*, 38: 3980-3992.
- Theis C (1935). "The relation between the lowering of the piezometer surface and the rate and duration of discharge of well using groundwater storage". *Am. Geophys. Union Trans.*, 16: 512-524.
- US, Salinity Laboratory Staff 1954. "Diagnosis and improvement of saline and alkali soil", U.S. Dept. Agric., Hand Book No.60, Washington, D.C., p. 160.
- Vega V, Pardo R, Barrado E, Deban L (1998). "Assessment of seasonal and polluting effects on the quality of river water by exploratory data analysis" *water research* 32: 3581-3592.
- Williams J (2001a). Salt balance in the Rio Grande project from San Marcial, New Mexico, to Fort Quitman, Texas. M.Sc. Thesis, New Mexico State University, Las Cruces, NM.
- Wilson J, Guan H (2004). Mountain block hydrology and mountain front recharge. In: Hogan JF, Phillips FM, Scanlon BR (eds) *Groundwater recharge in a desert environment: the southwestern United States*. AGU, Washington, DC, pp. 113-137.
- Wunderlin D, Diaz M, Ame M, Pesce S, Hued A, Bistoni M (2001). "Pattern recognition techniques for the evaluation of spatial and temporal variations in water quality" A case study: Suquia river basin (Cordoba- Argentina), *Water Res.*, 35: 2881-2894.